Surface Properties of Poly[2-(perfluorooctyl)ethyl acrylate] Deposited from Liquid CO_2 High-Pressure Free Meniscus Coating

Jaehoon Kim, Kirill Efimenko, Jan Genzer, and Ruben G. Carbonell*

Department of Chemical and Biomolecular Engineering, North Carolina State University, Raleigh, North Carolina 27606-7905

Received October 16, 2006; Revised Manuscript Received November 9, 2006

ABSTRACT: The surface characteristics of poly[2-(perfluorooctyl)ethyl acrylate] (PFOEA) films deposited using a high-pressure free meniscus coating (hFMC) process with liquid CO_2 (l-CO_2) as the coating solvent on 12.5 cm diameter silicon wafer substrates were investigated using contact angle measurements, atomic force microscopy (AFM), X-ray photoelectron spectroscopy (XPS), and near-edge X-ray adsorption fine structure (NEXAFS) spectroscopy. The results were compared with surface property measurements of PFOEA films deposited from 1,1,2-trichlorotrifluoroethane (Freon 113) under normal dip coating conditions at atmospheric pressure. NEXAFS measurements showed that perfluoroalkyl groups in the films from l-CO_2 and Freon 113 were well-organized and oriented normal to the substrate at the air/polymer interface. AFM images and XPS measurements revealed that a terrace-like structure of the PFOEA film from l-CO_2 resulted in carbonyl group exposure at the air/polymer interface. This leads to smaller contact angles on the films cast from l-CO_2 relative to the specimens deposited from Freon 113. Annealing the films deposited from the solvents resulted in droplet formation on the surface due to dewetting. The critical surface tension (γ_c) after annealing the film prepared from Freon 113 increased from 6.5 to 8.5 mJ/m^2, whereas γ_c of the film deposited from l-CO_2 decreased slightly from 9.7 to 8.9 mJ/m^2. We discuss how surface morphology changes before and after annealing play a role in the variation of γ_c.

1. Introduction

Surface properties of polymer films, including surface morphology and roughness, are often critical to their applications, particularly for use in optical, adhesive, frictional, and biocompatible devices. For example, it is well-known that surface roughness plays an important role in determining the wettability of polymer surfaces.[1−3] In addition, the surface morphology of electrically conductive films influences their functionality.[4,5] Morphology and roughness characteristics of polymer films are known to be highly dependent on sample preparation history, in particular, on the evaporation rate of the casting solvents in solution-based coating techniques.[6−8] Rapid evaporation of solvent causes thin film instabilities, such as thermal, surface tension, and/or convection driven flows, resulting in detrimental effects on surface uniformity and film quality. Another source of film roughness during solvent evaporation is crust formation, which can lead to uncontrollable film morphologies.[9] In order to minimize the occurrence of such unfavorable surface effects, it is important to control solvent evaporation rates during and after coating of polymer films.

It has been shown[10] that high-quality ultrathin poly[2-(perfluorooctyl)ethyl acrylate] (PFOEA) films can be deposited on a silicon wafer substrate by using high-pressure free meniscus coating (hFMC) with liquid carbon dioxide (l-CO_2) as a coating solvent. The control of the evaporation rate of l-CO_2 during film deposition resulted in highly uniform films with low surface root-mean-square (rms) roughness (≈2 nm) and few "drying defects". This paper examines the unique surface properties of the PFOEA films obtained from l-CO_2 hFMC. The wettability, morphology, and surface structure of the films are probed by using contact angle measurements, atomic force microscopy (AFM), X-ray photoelectron spectroscopy (XPS), and near-edge X-ray adsorption fine structure (NEXAFS) spectroscopy. The surface properties of the PFOEA films deposited from l-CO_2 are compared with the surface properties of PFOEA films deposited from 1,1,2-trichlorotrifluoroethane (Freon 113) under normal dip coating conditions at atmospheric pressure with no control on the evaporation rate. In addition, it is shown that dewetting of PFOEA films takes place when the films are annealed above the mesomorphic/isotropic phase transition temperature of PFOEA (≈77 °C).[11] This phase transition of PFOEA is due to the side chain crystallization of the long perfluoroalkyl groups at high temperatures. The surface properties of the annealed films are compared to the surface properties of nonannealed films cast from l-CO_2 and Freon 113.

* Corresponding author: e-mail ruben@ncsu.edu, tel 1-919-515-5118.

2. Experimental Section

2.1. Materials, Polymerization, and hFMC. 2-(Perfluorooctyl)-ethyl acrylate monomer ($H_2C{=}CHCO_2(CH_2)_2(CF_2)_8F$) (FOEA) was obtained from Daikin Co. (Osaka, Japan). 1,1,2-Trichlorotrifluoroethane (Freon 113) (HPLC grade) was purchased from Fisher Scientific (Pittsburgh, PA). Azobis(isobutyronitrile) (AIBN), methanol, and ethanol were purchased from Sigma-Aldrich (St. Louis, MO). The substrates were 12.5 cm diameter type ⟨100⟩ silicon wafers purchased from Silicon Valley Microelectronics, Inc. (San Jose, CA). The native silicon oxide layer thickness determined by ellipsometry was 20.64 ± 0.83 Å. The 600 μm thick wafers were single-side polished. The CO_2 was Coleman grade (purity of 99.99%) contained in a high-pressure tank with no helium headspace obtained from National Welders (Charlotte, NC).

Poly[2-(perfluorooctyl)ethyl acrylate] (PFOEA) was synthesized by homogeneous free-radical polymerization in supercritical carbon dioxide (scCO_2) in a 1200 mL reactor using 1% AIBN as initiator at 20.69 MPa and 60 °C for 24 h. The reaction mixture was dissolved in Freon 113, and the polymer was precipitated twice in methanol and dried in a vacuum oven at 40 °C for 48 h. The molecular weight of the polymer was 26 000 g/mol, determined by gel permeation chromatography (GPC) with a trifluorotoluene as the mobile phase. The measured polydispersity index for the polymer was 1.9.

10.1021/ma0623791 CCC: $37.00
Published on Web 01/06/2007

All of the coating experiments were carried out using a large scale high-pressure free meniscus coating (hFMC) apparatus. The details of the construction of this apparatus and the coating procedures have been fully discussed in a previous paper.[12] Using this high-pressure free meniscus coating process, it was possible to control the withdrawal velocity, the polymer solution concentration in l-CO_2, and the rate of evaporation of carbon dioxide from the film by adjusting the pressure difference between the chamber and the vapor pressure of liquid carbon dioxide. The following nomenclature will be used in this paper to describe the coating conditions of a given sample: 5 wt %−0.12 cm/s−l-CO_2 represents a PFOEA film deposited by hFMC on a silicon wafer using a 5 wt % solution of PFOEA in l-CO_2, a withdrawal velocity (U_w) of 0.12 cm/s, and an evaporation driving force of 0 psi. The evaporation driving force in the l-CO_2 hFMC process represents the difference between the solution vapor pressure and the pressure in the coating vessel (ΔP).[12,13] The nomenclature 1 wt %−0.12 cm/s−Freon 113 designates a PFOEA film deposited from Freon 113 using a 1 wt % solution of PFOEA in Freon 113 and a withdrawal velocity U_w of 0.12 cm/s in the same coating apparatus, but at ambient conditions with no control on the evaporation rate of the solvent. Using this nomenclature, 5 wt %−0.12 cm/s−l-CO_2−anneal and 1 wt %−0.12 cm/s−Freon 113−anneal refer to the corresponding films deposited from l-CO_2 and Freon 113, respectively, that have been annealed above the isotropization temperature (≈77 °C).[11] The annealing was carried out in a vacuum oven at 120 °C for 12 h. The pressure in the oven during annealing was less than 1 Torr.

2.2. Characterization. The thickness of all films deposited on the silicon wafer substrates was measured by ellipsometry using variable-angle spectroscopic ellipsometer (VASE, J. A. Woollam, Co., Inc., Lincoln, NE). The surface morphology of the coatings was observed using atomic force microscopy (AFM) with a Digital Instrument Dimension 3000 equipped with a Nanoscope IIIa controller (Santa Barbara, CA) and a vibration-shielded hood. A special image processing software (Matrox Inspector, Matrox Electronic Systems Ltd., Canada) was used to estimate the areas of droplets resulting from dewetting of the annealed films. The droplet regions were defined as those portions of the surface where the gray scale value was more than a threshold value. The setting of the threshold value was dependent on the extent of grayness of a given image. The image processing software was used to filter the images and to determine the area of pixels that met the given gray scale threshold value.

Contact angle measurements were performed using a Ramè-Hart contact angle goniometer (model 100-00, Ramè-Hart, Mountain Lakes, NJ) equipped with a CCD camera. The captured image was analyzed using the software provided by Ramè-Hart. The advancing contact angles were measured by slowly injecting 8 μL of the probe liquid; the receding contact angles were measured by removing 4 μL of liquid from the droplet. The contact angles reported in this paper represent average values over four measurements performed on each sample. A series of linear *n*-alkanes including *n*-hexane (surface tension γ_l = 18.4 mJ/m^2), *n*-heptane (γ_l = 20.1 mJ/m^2), *n*-octane (γ_l = 21.6 mJ/m^2), *n*-decane (γ_l = 23.8 mJ/m^2), and *n*-dodecane (γ_l = 25.4 mJ/m^2)[14] were used as standards to construct a Zisman plot.[15] In addition, diiodomethane (γ_l = 50.8 mJ/m^2) and water (γ_l = 72.8 mJ/m^2) were used to compare the measured contact angles with literature values.

X-ray photoelectron spectroscopy (XPS) measurements were carried out using a Physical Electronics model 5400 (Chanhassen, MN) spectrometer equipped with a hemispherical capacitor analyzer. A monochromatic Al K$\alpha_{1,2}$ source was used to irradiate a 1 mm diameter spot on each sample at 15 kV, 500−600 W, and 35−40 mA. The pressure in the chamber was maintained below 2 × 10^{-8} Torr during the measurement. All binding energies are referenced to a C 1s neutral carbon peak at 285.0 eV to compensate for surface charging effects. All data were collected at two different takeoff angles between the sample and analyzer (40° and 75°). The approximate sampling depths at 40° and 75° takeoff angles are 4.4 and 6.6 nm, respectively. These sampling depth values were calculated using an estimation of the C 1s inelastic mean free path of 2.3 nm with the Ashley method.[16] The PFOEA repeat unit density of 1.847 g/cm^3, valence electrons of 190, and molecular weight of 518.15 g/mol were used for the calculation of the C 1s inelastic mean free path. The unit density was estimated using a group contribution method.[17] C 1s high-resolution peak spectra were deconvoluted using a XPSPEAK 4.1 curve-fitting software assuming 50% Lorentzian−Gaussian peaks and a Shirley background over the energy range of the peak.

Near-edge X-ray adsorption fine structure (NEXAFS) experiments were carried out at the National Synchrotron Light Source in the Brookhaven National Laboratory. A detailed description of the instrument can be found elsewhere.[18,19] The X-ray beam, ≈85% polarized, irradiated about 1 mm^2 area on the specimen. Polarization-dependent spectra were collected at two different incident angles: normal X-ray incidence to the substrate (θ = 90°) and grazing X-ray incidence to the substrate (θ = 20°). The normal and grazing X-ray incidence geometries correspond to the electric field vector **E** parallel to the substrate and to **E** tilted from the surface normal, respectively. The absorption spectra are due to excitation of core level electrons to unoccupied antibonding molecular orbitals (1s → σ* or 1s → p*) by absorbing incident X-rays. The corresponding excitation gives rise to intense resonances in the spectra. The partial electron yield (PEY) signal from elastically emitted Auger electrons at only the topmost surface region was collected using a channeltron electron multiplier with an adjustable entrance grid bias. The sampling depth of the PEY signal is in the range 1.5−2 nm.[20] The PEY signals were normalized to the incident photon beam. An important issue concerning the study of organic materials is the possibility of sample damage during the characterization with UV light, X-rays, and electron radiation. Semifluorinated materials are particularly sensitive to these effects.[21−23] In order to test sample damage due to X-ray beam during the NEXAFS experiments, NEXAFS scans were rerun on the same sample; NEXAFS spectra showed no damage effects for at least three consecutive runs taken from the same spot on the sample.

Table 1. Comparison of Physical Properties of Coating Solvents and the Average Dry Film Thickness (H_{dry})

	density[a] (g/cm^3)	viscosity[a] (cP)	surface tension[a] (mJ/m^2)	av H_{dry} (Å)
l-CO_2	0.91	0.0951	4.08	241[b]
Freon 113	1.625	0.92	19.8	276[c]

[a] Properties at 2.5 °C.[52] [b] Coating conditions: solution concentration of 5 wt %, withdrawal velocity of 0.12 cm/s, no evaporation driving force, and 2.5 °C. [c] Coating conditions: solution concentration of 1 wt %, withdrawal velocity of 0.12 cm/s, and 2.5 °C.

3. Results and Discussion

3.1. Thickness and Morphology Comparison of PFOEA Films from l-CO_2 and Freon 113. Table 1 lists the physical properties of the coating solvents and the average dry film thickness (average H_{dry}) of PFOEA films coated from l-CO_2 and Freon 113 measured via ellipsometry as described in the Characterization section. The density of l-CO_2 at 2.5 °C is 0.91 g/cm^3. This value is comparable to the density of most typical organic solvents, except for the unusually dense fluorinated solvents such as Freon 113. In contrast, l-CO_2 has a much lower viscosity compared to those of typical organic solvents. For example, the viscosity of 1-CO_2 at 2.5 °C is 0.0951 cP, which is an order of magnitude smaller than the viscosity of Freon 113. l-CO_2 also exhibits a very low surface tension; at 2.5 °C, γ_{l-CO2} = 4.08 mJ/m^2, a value that is ∼5 times smaller than the surface tension of Freon 113. The low viscosity of l-CO_2 results in much thinner films during free meniscus coating (dip coating) because the viscous drag forces in the film entrainment region are weaker than those of the organic solvent. The entrained liquid film thickness in a dip coating process is approximately

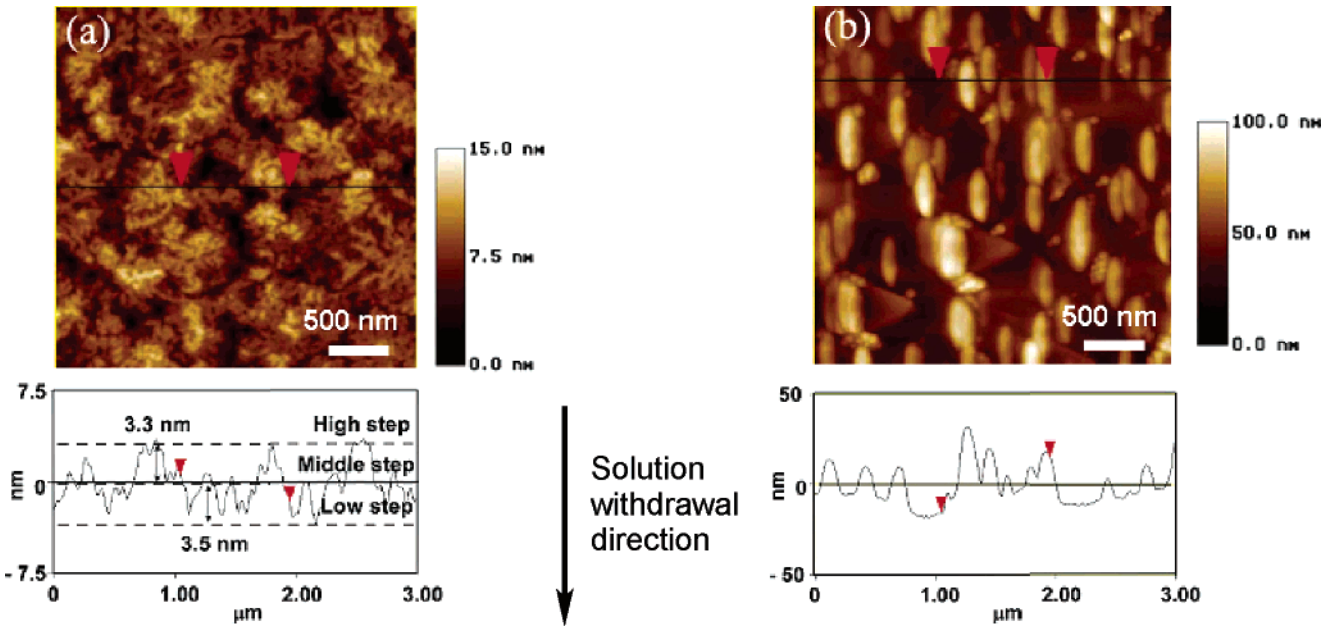

Figure 1. AFM images and cross-sectional profiles of (a) 5 wt %−0.12 cm/s−l-CO_2 (scanning area: 3 μm × 3 μm, height scale: 15 nm), (b) 1 wt %−0.12 cm/s−Freon 113 (scanning area: 3 μm × 3 μm, height scale: 100 nm); depressions, dark; peaks, bright.

proportional to the 2/3 power of the solution viscosity in the low capillary number regime.[24] As a result, a 5 times larger polymer concentration in the l-CO_2 solution resulted in film thicknesses comparable to the average H_{dry} of the film coated from Freon 113 solution at the same withdrawal velocity with no evaporation driving force, as shown in Table 1.

Atomic force microscopy (AFM) was used to gain information about the morphology of the PFOEA films deposited from l-CO_2 and from Freon 113. Figure 1 contains AFM images (scanning area: 3 μm × 3 μm) and surface cross-sectional profiles of the PFOEA films from l-CO_2 and from Freon 113 that were collected at the center of the substrate. The AFM image of the 5 wt %−0.12 cm/s−l-CO_2 sample demonstrates that highly uniform PFOEA films can be produced by the hFMC process using l-CO_2 (cf. Figure 1a). The film exhibits a dendritic or fractal structure. The average rms roughness of the PFOEA films from l-CO_2 is only 1.97 ± 0.10 nm. These very low rms roughness values result primarily from the ability to decouple the film formation and films drying processes during the 1-CO_2 hFMC deposition procedure. In contrast, the PFOEA films deposited from Freon 113 exhibit more nonuniform surface morphologies. Figure 1b shows an AFM image of the film deposited from Freon 113 taken with the alignment in the direction of film entrainment. It can be seen that oval polymer aggregates ≈500 nm long and 100 nm wide are deposited on the surface. The height of these aggregates is in the range of 35−60 nm. The triangular shadows trailing the aggregates in Figure 1b are an imaging artifact caused by the scanning line direction. The presence of polymer aggregates results in a rms roughness of 16.0 ± 2.7 nm, a value that is approximately an order of magnitude larger than the rms roughness of films deposited from l-CO_2. The formation of these PFOEA aggregates results primarily from the rapid and uncontrollable evaporation rate of the organic solvent during film entrainment and drying steps in the dip coating process.

3.2. Comparison of Surface Structure and Wettability of PFOEA Films from l-CO_2 and Freon 113. Poly(perfluoroalkyl) acrylates and poly(perfluoroalkyl) methacrylates with long perfluoroalkyl chains (e.g., $F(CF_2)_n$ with $n > 7$) are known to undergo chain crystallization, resulting in single or double layer packing of the side chains in the polymer matrix.[25] Therefore, in addition to the glass transition temperature (52 °C in the case of PFOEA), these polymers exhibit a mesomorphic/isotropic phase transition temperature. X-ray diffraction studies have revealed that PFOEA films exhibit a high degree of bilayer structure below the phase transition temperature (≈77 °C).[11] This bilayer structure is due to the vertical alignment of neighboring perfluoroalkyl groups.[26,27] The single bilayer length of PFOEA, determined by its X-ray diffraction pattern, is 3.32 nm, a value which is slightly smaller than the bilayer length estimated using a space-filling molecular model (3.6 nm).[27]

The surface chemical compositions of the PFOEA films deposited from l-CO_2 and from Freon 113 were examined using X-ray photoelectron spectroscopy (XPS); representative spectra are shown in Figure 2. Even though PFOEA has nine chemically different types of carbon, six peaks were sufficient to deconvolute the C 1s high-resolution spectra: the aliphatic carbons with a binding energy of 285.0 ± 0.1 eV, the carbon atom bonded to the carbonyl carbon (*C*HC═O) at 285.7 ± 0.1 eV, the ether carbon (*C*−O) at 287.1 ± 0.1 eV, the carbonyl carbon (*C*═O) at 289.1 ± 0.1 eV, the carbon atom with two bonds with fluorine (*C*F_2) at 291.3 ± 0.1 eV, and the carbon atom with three fluorine bonds (*C*F_3) at 293.4 ± 0.1 eV. These maximum binding energies agree well with previously reported values.[16,28,29] Figure 2 shows the high-resolution XPS C 1s spectra and peak deconvolution fittings of the 5 wt %−0.12 cm/s−l-CO_2 sample at two different takeoff angles of 40° and 75° between sample and analyzer. In angle-resolved XPS, the surface sensitivity is enhanced at low takeoff angles while the bulk sensitivity is enhanced at higher takeoff angles. The relative areas of the fluorinated carbon species (CF_2 and CF_3) decrease with increasing takeoff angles, indicating surface enrichment of the perfluoroalkyl groups. This surface segregation of fluorine-based species is a well-known and documented phenomenon;[29−31] it results from the tendency of the polymer films to minimize their overall free energy by allowing low-energy constituents to enrich the free surface.

Table 2 lists the functional group composition of fluorinated carbons (−CF_3 and −CF_2) and carbonyl carbon (⟩C═O) of the PFOEA films coated from l-CO_2 and from Freon 113 as

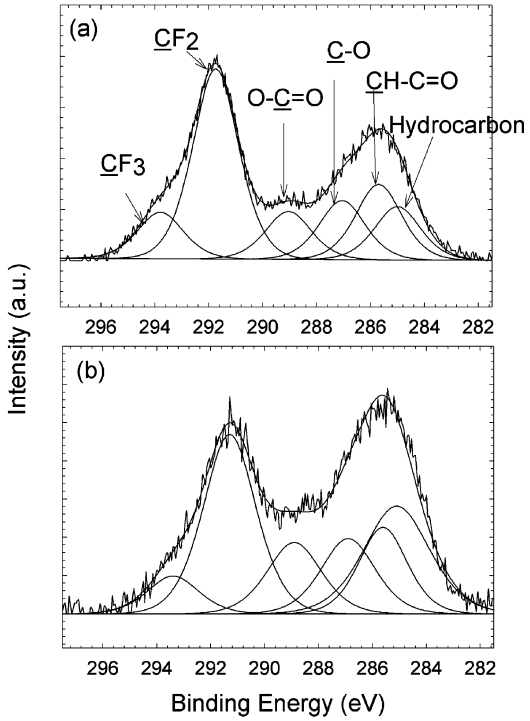

Figure 2. High-resolution XPS C 1s spectra and peak fittings of the PFOEA film deposited from l-CO_2 hFMC at takeoff angle of (a) 40° and (b) 75°.

Table 2. Functional Group Compositions of 5 wt %−0.12 cm/s−l-CO_2 and 1 wt %−0.12 cm/s−Freon 113 at the Takeoff Angle of 40°

	calcd value (%)	5 wt %−0.12 cm/s−l-CO_2 (%)	1 wt %−0.12 cm/s−Freon 113 (%)
$-CF_3$	7.70	9.80	9.60
$-CF_2-$	53.80	48.25	52.87
⟩C═O	7.70	11.50	6.94

estimated from the high-resolution XPS C 1s spectra at a takeoff angle of 40°. These values are compared to the calculated average functional group composition values of the polymer. The atomic composition of the $-CF_3$ group at the topmost layer in the film formed from l-CO_2 is slightly higher than the calculated average $-CF_3$ composition. However, the atomic composition of $-CF_2-$ groups in the film from l-CO_2 is lower relative to the calculated value. Furthermore, the experimentally observed atomic concentration of the ⟩C═O group is ∼11.5%; this value is larger than the calculated (∼7.7%). The topmost chemical composition of the PFOEA film deposited from Freon 113 is different from that of the film prepared using l-CO_2. The atomic composition of the $-CF_2-$ moiety in the film deposited from Freon 113 is comparable to the average calculated value while the atomic composition of the ⟩C═O group is smaller than the calculated value. This trend is in accord with the results reported previously by Tsibouklis et al.,[32] who studied the XPS spectra of PFOEA films prepared by dip coating with Freon 113 and also observed that the experimentally measured content of ⟩C═O was lower than the calculated value. The surface energy of the film was found to be as low as 6.9 mJ/m^2, suggesting that the perfluoroalkyl groups were oriented normal to the substrate, thereby exposing the $-CF_3$ groups to the free surface.[32] The lower content of $-CF_2-$ and the more abundant presence of the ⟩C═O group in the film deposited from l-CO_2 (relative to the calculated values) indicate that the perfluoroalkyl moieties in the film from l-CO_2 are not oriented perfectly normal to the substrate and that some carbonyl groups are exposed at the topmost layers. The validity of this preliminary interpretation can be examined by measuring the side chain orientation of the PFOEA films.

The perfluoroalkyl group orientation of the PFOEA films from l-CO_2 and from Freon 113 at the topmost layers was further examined using near-edge X-ray adsorption fine structure (NEXAFS) spectroscopy. Figure 3a,b present partial electron yield (PEY) NEXAFS spectra at the carbon K-edge of the films deposited from l-CO_2 and from Freon 113 measured at the grazing X-ray incidence ($\theta = 20°$, dashed line) and normal X-ray incidence ($\theta = 90°$, solid line) geometries. The sharp resonance intensity at around 288 eV corresponds to the 1s → π^* transition of the C═O group. Resonance intensities at ∼292 and ∼295 eV originate from the 1s → σ^* transitions in the C−F and C−C bonds, respectively. The signal at 298 eV represents a complementary C−F resonance to the one found at 292 eV. These peak assignments agree well with those in the literature.[33−37] Resonance intensity is maximized when a given antibonding orbital is oriented parallel to the oscillating direction of the electric field **E** due to the fact that the excitations are dominated by the dipole selection rule. Recognizing that the σ^* orbitals are oriented parallel to the corresponding σ bond and considering that the resonance intensity of the 1s → σ_{C-F}^* transition is larger at $\theta = 90°$ than that at $\theta = 20°$ reveals that C−F σ bonds are oriented roughly parallel to the substrate. The opposite polarization dependence of the 1s → σ_{C-C}^* transition with the incidence angles suggests that the C−C bonds in the perfluorinated side chain are oriented approximately normal to the substrate. This indicates that the perfluoroalkyl groups in the film cast from l-CO_2 are oriented preferentially normal to the interface on the free surface. This observation appears to be at odds with the atomic composition estimation results from the XPS spectra. The larger atomic composition of the ⟩C═O group than the calculated value means that, at least as a first approximation, the ⟩C═O groups might be exposed at the interface.

This apparent discrepancy can be resolved by considering the surface morphology of the film. Even though the molecular scale morphology of polymers containing long perfluoroalkyl group is highly regular due to hexagonal packing of the side chains,[38] the microscopic morphology is not uniform. For example, spin-coated films of such fluoropolymers, and other side-chain liquid crystalline polymers, exhibit small holes with a diameter of 10−100 nm and a characteristic depth approximately equal to the bilayer length of the polymer chains.[27,39−41] The hole formation in these systems has been explained by lateral shrinkage of the topmost surface layer due to closer side-chain packing after evaporation of solvent or by insufficient material for complete coverage of the topmost layers.

The AFM image and a cross-sectional surface profile along the line indicated in Figure 1a reveal that the PFOEA films from l-CO_2 do not contain holes but adopt a "terrace-like" structure. The shapes of the terraces at each step are highly irregular, and the terraces are well connected. As shown in the surface profile, the height difference between the terraces is in the range 3.3−3.5 nm. These values agree well with the single bilayer length determined by X-ray diffraction and the space-filling model (3.3−3.6 nm).

Figure 4a depicts a schematic representation of a putative PFOEA film structure deposited from l-CO_2 hFMC, as deduced from the discussion thus far. This arrangement can help explain the presence of the ⟩C═O groups at the topmost layer. At each end of the terraces, the ⟩C═O groups are exposed to the air/surface interface. As a result, incoming X-rays can detect the

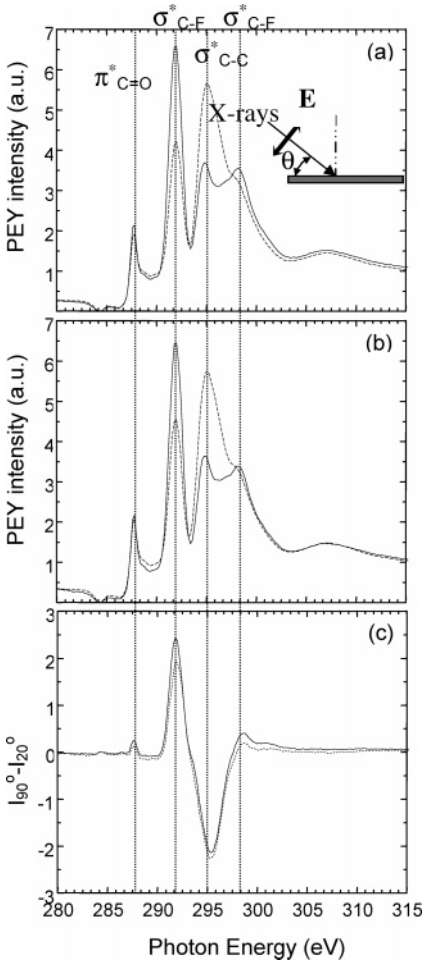

Figure 3. PEY NEXAFS spectra from (a) 5 wt %−0.12 cm/s−l-CO_2 and (b) 1 wt %−0.12 cm/s−Freon 113 at two different sample orientation with respect to the incident X-ray beam, θ (dashed line: $\theta = 20°$; solid line: $\theta = 90°$). (c) PEY intensity from the two different incident angle difference (dashed line: 1 wt %−0.12 cm/s−Freon 113; solid line: 5 wt %−0.12 cm/s−l-CO_2).

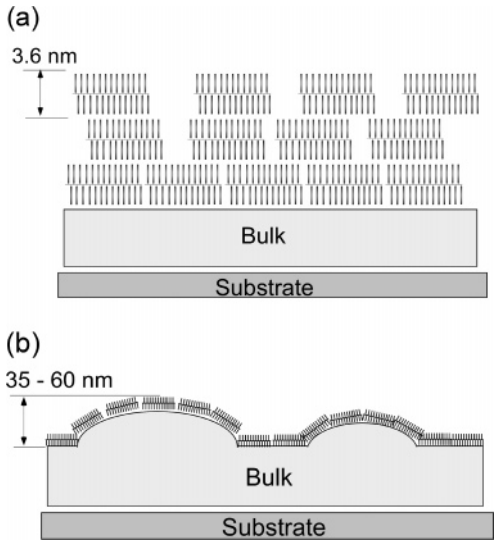

Figure 4. Schematic representation of structure in (a) 5 wt %−0.12 cm/s−l-CO_2 and (b) 1 wt %−0.12 cm/s−Freon 113 films.

⟩C═O groups at each end of the terrace. This is consistent with the higher experimental atomic composition of the ⟩C═O group relative to the calculated value, even though perfluoroalkyl groups are well-oriented normal to the substrate.

Figure 3b shows that perfluoroalkyl chains of the film from Freon 113 are also oriented normal to the substrate. However, the polarization dependence of the PEY NEXAFS spectrum of the PFOEA film cast from Freon 113 is slightly weaker than that of the film cast from l-CO_2. The difference plot of intensities at $\theta = 90°$ and $\theta = 20°$ ($I_{90°} - I_{20°}$) of the films from l-CO_2 and from Freon 113 is shown in Figure 3c. This difference plot can be used as a qualitative indicator of the degree of orientation of the perfluoroalkyl groups at the free surface. The intensity differences of peaks corresponding to the 1s → σ_{C-F}* transitions in the film cast from Freon 113 are smaller than those in the film from l-CO_2. This reveals that the perfluoroalkyl groups at free surface of the Freon 113 cast film are less oriented than those of the film deposited from l-CO_2. However, the surface morphology difference of the films from l-CO_2 and from Freon 113 should be taken into account.

As discussed previously, oval polymer aggregates ∼500 nm long and 100 nm were detected in the film cast from Freon 113. The top of each aggregate is likely covered with perfluoroalkyl groups that are oriented perpendicularly to the surface, but perfluoroalkyl groups in other regions of the aggregates are not likely oriented perpendicular to the substrate. The XPS results on the film from Freon 113 support this hypothesis. The fact that the measured atomic composition of the ⟩C═O group is lower than the calculated value indicates surface aggregation of perfluoroalkyl groups at the topmost layers. Figure 4b depicts a schematic representation of a putative structure of films deposited from Freon 113. The polarization dependence of the perfluoroalkyl groups oriented normal to one side of the hills may cancel out that of the perfluoroalkyl groups oriented normal to the other size of the hills. Therefore, the perfluoroalkyl groups oriented normal to the hills do not strongly contribute to the polarization dependence of the PEY intensities. More quantitatively, ∼7.7% more electrons in the C−F groups of the film from Freon 113 are excited to the incident X-rays at $\theta = 20°$ and ∼2.2% fewer electrons are excited to the incident X-rays at $\theta = 90°$ compared with the film cast from l-CO_2. This leads to approximately a 20% decrease in the angular dependence of the 1s → σ_{C-F}* resonance peak of the film from Freon 113, implying that ∼20% of the perfluoroalkyl groups at the topmost layers do not contribute to the polarization dependence. The percentage of the total area covered by the polymer aggregates is ∼29%, a value which is larger than the amount of decrease in the polarization dependence. This is probably due to the presence of the perfluoroalkyl groups residing at the top of each polymer aggregate. Thus, all these observations provide evidence that the perfluoroalkyl groups are oriented normal to the substrate.

Table 3 shows a comparison of the coating conditions, rms roughness, contact angles of water and diidomethane, and contact angle hysteresis of PFOEA films deposited by different group using dip coating with a variety of solvents. Regardless of the dip coating conditions, contact angles of the test liquids on the PFOEA films from the organic solvents are higher than those of the PFOEA film from l-CO_2. At least two possible reasons can be offered to explain this observation. First, it is well-known that the wettability of hydrophobic surfaces decreases with increased surface roughness. This influence of surface roughness on wettability was addressed by Wenzel[1] and later by Cassie and Baxter.[42,43] While in the Wenzel regime the liquid drop penetrates into the gaps between asperities, in the Cassie−Baxter regime the liquid drop does not penetrate into the asperities as gas molecules are trapped beneath the drop. Marmur has reported that the Wenzel regime dominates when

Table 3. Comparison of Coating Conditions, Surface Roughness, and Contact Angles of PFOEA Films

dip coating conditions (concn, withdrawal velocity)	solvent	rms roughness (nm)	contact angles (deg) (hysteresis (deg)) water	contact angles (deg) (hysteresis (deg)) diiodomethane	ref
0.2 wt %, 1 cm/s	1,1,1,3,3,3-hexafluoro-2-propanol	NA[a]	117[b]	NA[a]	53
0.13 wt %, 8×10^{-4} cm/s	Freon 113	NA[a]	120[c]	NA[a]	27
0.4 wt %, 1 cm/s	Freon 113	NA	114[d]	105[c]	54
0.1 wt %, 1 cm/s	Freon 113	9.6	117[d] (8)	112[d] (12)	47
1 wt %, 0.12 cm/s	Freon 113	14.0	118[d] (19)	105[d] (15)	this study
5 wt %, 0.12 cm/s	l-CO_2	1.45	111[d] (8)	100[d] (3)	this study

[a] Not available. [b] Receding contact angle. [c] Average values of advancing and receding contact angles. [d] Advancing contact angles.

Table 4. Comparison between Intensity Difference of the 1s → σ_{C-F}* Resonance Peak in NEXAFS Determined from the NEXAFS Difference Plots and PFOEA Aggregate Area

	intensity difference (au)	intensity decreases (%)	PFOEA aggregate (or droplet) area (%)
5 wt %−0.12 cm/s−l-CO_2	2.3735		
1 wt %−0.12 cm/s-Freon 113	1.9062	20	29
5 wt %−0.12 cm/s−l-CO_2-anneal	2.0086	15	16
1 wt %−0.12 cm/s−Freon 113−anneal	1.9306	19	18

the droplet size is 2−3 orders of magnitude larger than the roughness scale.[44,45] Since the dimensions of the oval-like structures in the PFOEA films prepared from Freon 113 are 3−4 orders of magnitude smaller than the size of the test liquid droplets and the density of the structure is low, the liquid drop may penetrate into the corrugated surface of the film.[44,45] In the Wenzel regime, the relation between the contact angle on a smooth surface (θ_0) and the contact angle on the actual surface (θ) is given by[1]

$$\cos\theta = \frac{A}{A_0}\cos(\theta_0) = r\cos(\theta_0)$$

where A is the actual area, A_0 is the projected area, and r is the Wenzel roughness factor. The experimental as well as theoretical works of Wenzel on the effects of roughness on contact angles on low-energy surfaces (i.e., contact angles above 90°) show that the receding contact angle decreases and the advancing contact angle increases when r is smaller than 2.[1,2,46] The Wenzel roughness factor of the film deposited from Freon 113, calculated from the AFM images (assuming for simplicity that the polymer aggregates are hemispheres), is 1.38. Thus, the rough surface of the film from Freon 113 leads to a larger difference in advancing contact angles and receding contact angles (so-called contact angle hysteresis) as well as larger values of the advancing contact angles relative to those of the film cast from l-CO_2. Second, the surface morphology and side chain orientation of the films prepared from organic solvents and the film prepared from l-CO_2 are different. The wettability of polymers containing long perfluoroalkyl groups ($F(CF_2)_n$ with $n > 7$) is known to be extremely small because perfluoroalkyl groups are well-oriented at the topmost layer. As a result, well-oriented perfluoroalkyl groups inhibit the interaction of the more polar ⟩C═O moieties with the test liquids. As shown in Table 3, the water contact angle of the PFOEA film cast from l-CO_2 is 111°, which is 3−9° smaller than contact angles of films deposited from organic solvents. In fact, the water contact angle of the PFOEA film prepared from l-CO_2 is even smaller than those of polymer films with short perfluoroalkyl groups such as polyacrylate and polymethacrylate with C_6F_{13} side chains (115.9° and 114°, respectively),[28,47] even though the degree of orientation of the shorter perfluoroalkyl groups normal to the substrate is lower than that of the longer perfluoroalkyl groups at the topmost layer.[33] This is due to the fact that the ⟩C═O groups in the PFOEA film prepared from l-CO_2 is exposed at the interface, allowing polar interactions with the polar test liquid.

3.3. Effects of Annealing on Surface Morphology, Side-Chain Orientation, and Critical Surface Tension. Annealing of polymer films containing long perfluoroalkyl side chains in an air environment has been used to enhance surface enrichment of the perfluoroalkyl groups at the air/surface interface.[28,29] The PFOEA films deposited from l-CO_2 and from Freon 113 were annealed at 120 °C for 12 h in vacuum in order to promote surface segregation of the perfluoroalkyl groups to the interface. This annealing temperature is ∼40 °C above the isotropic temperature of PFOEA.[11] Morphology, side-chain orientation, and surface energy were measured on the annealed samples and compared with the surface properties of as-cast (nonannealed) specimens. Figure 5 shows AFM images (scanning area: 15 μm × 15 μm) of the nonannealed (as-cast) and the annealed samples. As discussed previously, the PFOEA film prepared from l-CO_2 is very uniform and exhibits a terrace-like structure with three different molecular scale step heights. As shown in Figure 5a, each terrace at the lower and higher step is well connected to its neighbors. The AFM images of the PFOEA films prepared from Freon 113 reveal that the surface comprises polymer aggregates with two different sizes: ∼500 nm long and 100 nm wide oval aggregates with 35−60 nm in height and 1−2 μm long and 1−2 μm wide aggregates with height of ∼500 nm (Figure 5b).

Upon annealing, the surface morphology of the film deposited from l-CO_2 changes dramatically due to film dewetting from the substrate. The surface exhibits small size droplets and large size droplets. The diameter of the small droplets is ∼1 μm, and the height is ∼50 nm. The small droplets coalesce to form large droplets during the annealing process. The diameter of the large droplets is ∼3 μm, and the height is ∼150 nm. The annealed sample of the film cast from Freon 113 exhibits morphologies similar to the specimen deposited from l-CO_2 except that the former has a larger number of small droplets (0.5−1 μm in diameter). Similar dewetting morphologies of long perfluoroalkyl group containing polymer films have been reported previously. These include films cast from poly[(perfluorooctyl)-ethyl methacrylate] (PFOEMA) on glass,[26] PFOEA films on poly(ethylene telephthalate) (PET),[48] and poly(benzyl ether) with perfluorooctyl ethyl groups on mica.[49] Sheiko et al. explained this peculiar dewetting behavior—low surface energy fluoropolymer dewetting on a high surface energy surface—by considering surface energy differences between the disordered

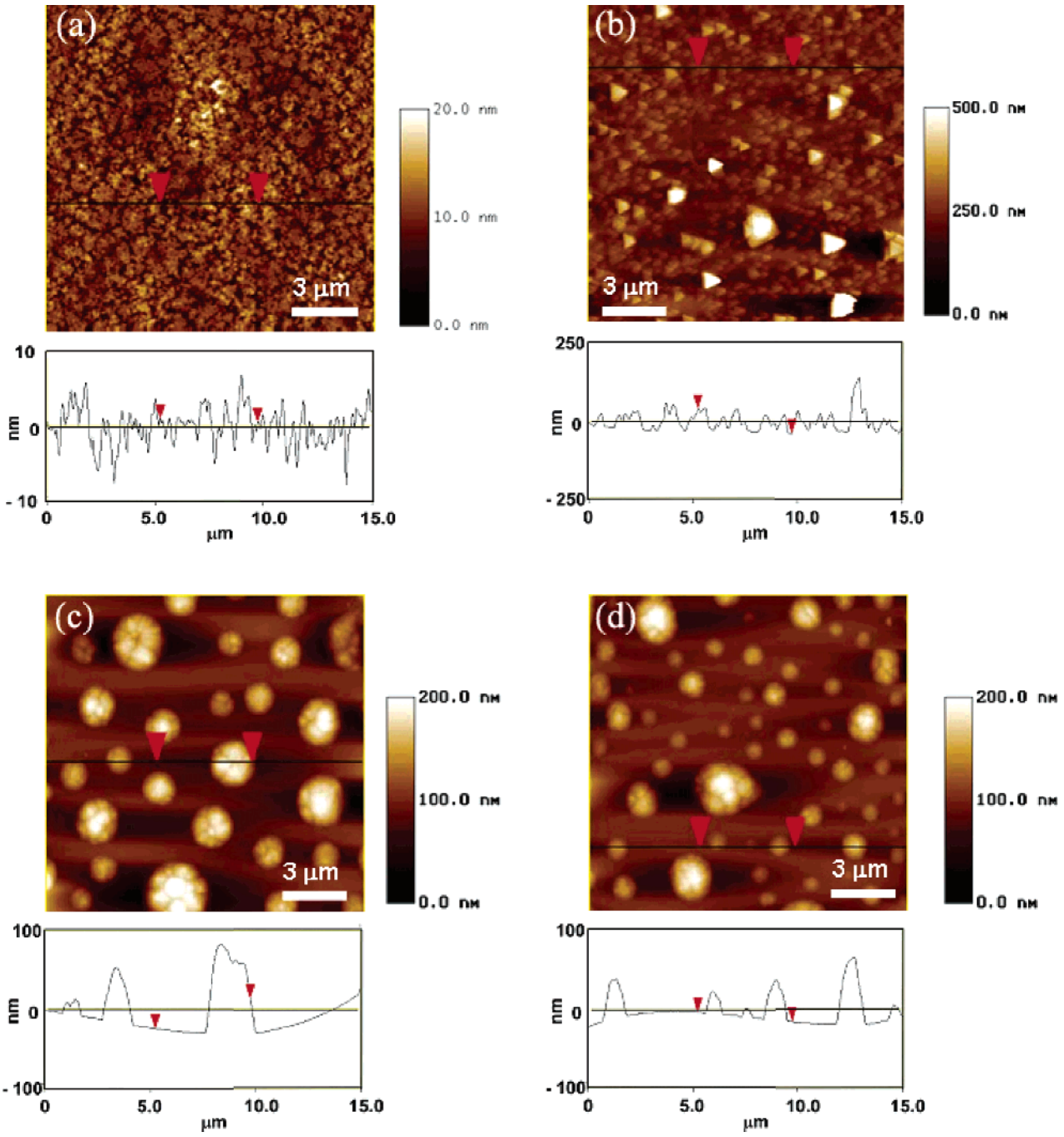

Figure 5. AFM images and cross-sectional profiles of (a) 5 wt %−0 psi−0.12 cm/s−CO_2 (height scale: 20 nm), (b) 1 wt %−0.12 cm/s−Freon 113 (height scale: 500 nm), (c) 5 wt %−0 psi−0.12 cm/s−CO_2−anneal (height scale: 200 nm), and (d) 1 wt %−0.12 cm/s−Freon 113−anneal (height scale: 200 nm). Scan area: 15 μm × 15 μm, depressions: dark, peaks: bright.

polymer melt and the ordered sublayers.[26] Sheiko et al. observed that during the dewetting of PFOEMA from glass the "open" area was covered with 1.5 monolayers of the polymer. AFM friction force tests of annealed poly[(perfluorooctyl)ethyl methacrylate] films on glass revealed that there was no friction contrast between the open area and droplets, suggesting that the open area and droplets had identical chemical composition and molecular orientation. Thus, PFOEMA thin film dewetting exhibits autophobic dewetting behavior.

Polymer coverage of the open area after annealing or autophobic dewetting of the PFOEA films can also be verified by using NEXAFS. Figure 6a,b depict PEY NEXAFS spectra collected at the carbon K-edge of the films prepared by casting from l-CO_2 and from Freon 113 after annealing, measured at incident X-ray angles of $\theta = 20°$ (dashed line) and $\theta = 90°$ (solid line). The droplet area in the annealed sample of the film formed by casting from l-CO_2 corresponds to ~16% of the total surface area, and the droplet area in the annealed sample of the film from Freon 113 corresponds to ~18% of the total surface area. Had the open area not been covered by the polymer, only the polymer in the droplets would have been excited by incident X-rays, and the intensities would have decreased significantly relative to the intensities collected from the nonannealed samples. However, the annealed samples exhibit comparable intensities to those of the nonannealed samples. This indicates that the open area is still covered with a thin polymer layer, and the perfluoroalkyl groups in the open area are well-oriented normal to the substrate. Table 4 lists the polarization dependence of the PEY NEXAFS spectra ($I_{90°} - I_{20°}$) of the 1s → σ_{C-F}* resonance peaks in the nonannealed and the annealed specimens.

Table 5. Surface Tension of Test Liquids at 20 °C, Contact Angles, and Hysteresis for the Test Liquids on 5 wt %−0 psi−0.12 cm/s−l-CO_2, 5 wt %−0 psi−0.12 cm/s−l-CO_2−Anneal, 1 wt %−0.12 cm/s−Freon 113, and 1 wt %−0.12 cm/s−Freon 113−Anneal

		5 wt %−0 psi−0.12 cm/s−l-CO_2		5 wt % -0 psi−0.12 cm/s−l-CO_2−anneal		1 wt %−0.12 cm/s−Freon 113		1 wt %−0.12 cm/s−Freon 113−anneal	
wetting liquids	surface tension (mJ/m^2)	advancing angle (deg)	hysteresis (deg)	advancing angle (deg)	hysteresis (deg)	advancing angle (deg)	hysteresis (deg)	advancing angle (deg)	hysteresis (deg)
n-hexane	18.4	54	3	57	10	62	13	58	7
n-heptane	20.1	63	3	64	7	68	14	64	9
n-octane	21.8	69	4	67	8	72	12	67	8
n-decane	23.8	72	3	74	7	77	11	74	7
n-dodecane	25.4	78	3	80	7	82	10	80	8
water	72.8	112	8	113	21	118	19	114	18

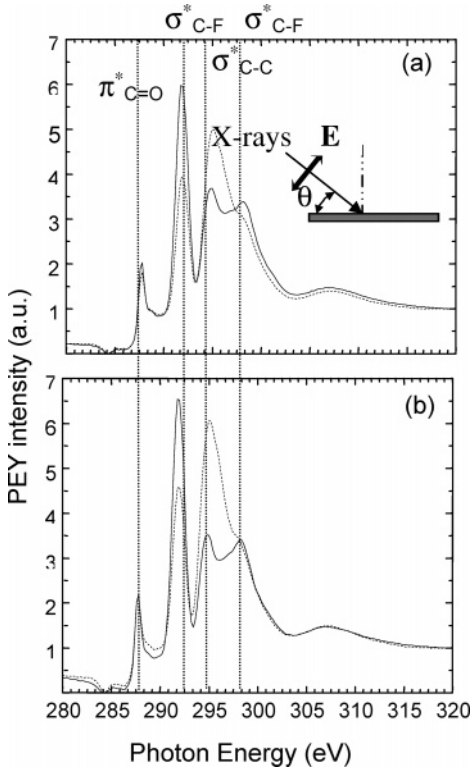

Figure 6. PEY NEXAFS spectra from (a) 5 wt %−0.12 cm/s−l-CO_2−anneal and (b) 1 wt %−0.12 cm/s−Freon 113-anneal at two different sample orientation with respect to the incident X-ray beam, θ (dashed line: $\theta = 20°$; solid line: $\theta = 90°$).

The substantial decrease in the $I_{90}°-I_{20}°$ of the film cast from Freon 113 relative to that of the film prepared from l-CO_2 (∼20%) was attributed to the presence of the oval-like polymer aggregates in the film cast from Freon 113. However, as discussed previously, the magnitude of the decrease in $I_{90}°-I_{20}°$ is smaller than the area of the polymer aggregates (∼29%). Again, the discrepancy between the polymer aggregate area in the film formed by casting from Freon 113 and the amount of decrease in $I_{90}°-I_{20}°$ is associated with the fact that polymers at the top of the semioval aggregates may contribute to the polarization dependence. In contrast, the decrease in $I_{90}°-I_{20}°$ of the annealed sample of the film formed from l-CO_2 is ∼15% and that of the annealed sample of the film cast from Freon 113 is ∼19%. As shown in Table 4, the degree of decrease in $I_{90}°-I_{20}°$ is comparable to the droplet areas of the annealed films. Thus, the comparability of the polymer droplet area in the annealed samples and the amount of decrease in $I_{90}°-I_{20}°$ reveals that the perfluorooctyl groups on the semispherical droplets do not contribute strongly to the polarization dependence.

Surface properties of the nonannealed samples and the annealed samples were further examined by measuring contact angles and by estimating critical surface tensions (γ_c). Values of γ_c of each film were calculated by extrapolating the linear fits of advancing contact angle data of *n*-alkanes to $\cos(\theta) = 1$. Figure 7 shows Zisman plots of the PFOEA films deposited from l-CO_2 and from Freon 113, before (solid symbols) and after (open symbols) annealing. Table 5 lists surface tensions of test liquids at 20 °C, advancing contact angles, and the contact angle hysteresis. The value of γ_c of the film deposited from Freon 113 is 6.5 mJ/m^2. This extremely low γ_c is due to the preferential segregation of the $-CF_3$ groups at the air/surface interface and the roughness of the film. Decreases in the advancing contact angles of the test liquids beyond the error range of contact angle measurement (±2°) were observed on the annealed film deposited from Freon 113. This resulted in a measured increase of γ_c to 8.5 mJ/m^2. Furthermore, contact angle hysteresis of the test liquids was found to decrease after annealing. The increase in γ_c and the decrease in the contact angle hysteresis after annealing of the film prepared from Freon 113 are due to a reduction in surface roughness; the Wenzel roughness factor in films cast from Freon 113 decreased from 1.38 to 1.18 after annealing. In contrast, as listed in Table 5, the advancing contact angles of the test liquids and the contact angle hysteresis increased slightly after annealing of the film prepared by casting from l-CO_2. The increases in the advancing contact angles of *n*-alkanes lead to a decrease in γ_c from 9.7 to 8.9 mJ/m^2 after annealing. The slight decrease in γ_c after annealing of the film cast from l-CO_2 is probably due to a decrease in the percentage of ⟩C═O groups present at the air/polymer interface and to a concurrent increase of surface roughness. The Wenzel roughness factor increased from 1 to 1.16 after annealing of the film deposited from l-CO_2. This causes a decrease in receding contact angles and a corresponding increase in contact angle hysteresis. Even though the receding

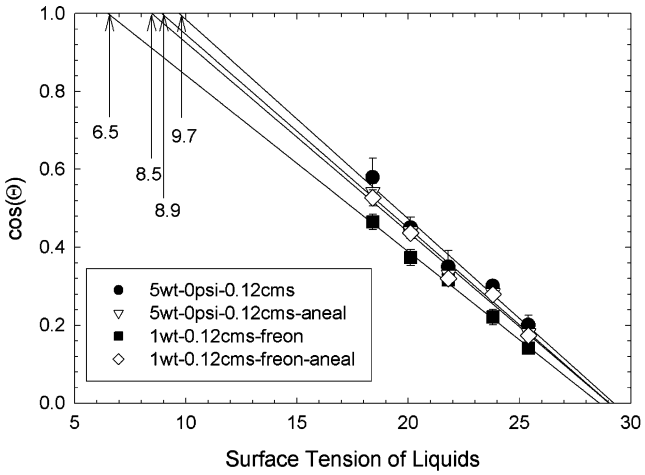

Figure 7. Zisman plot and critical surface tensions of 5 wt %−0.12 cm/s−l-CO_2, 1 wt %−0.12 cm/s−Freon 113, 5 wt %−0.12 cm/s−l-CO_2-anneal, and 1 wt %−0.12 cm/s−Freon 113−anneal.

contact angles decreased after annealing, the increase in surface roughness does not play an important role in increasing advancing contact angles. Ishikawa et al. observed similar trends in changes of contact angles after annealing of PFOEA films on PET. The advancing contact angle of water did not change significantly while the receding contact angle decreased ~30° after annealing.[48] Sheiko et al. found no significant changes in advancing contact angles of *n*-hexadecane on spun-cast poly-[(perfluorooctyl)ethyl ethacrylate] after annealing.[26] Since surface roughness always causes an increase in contact angle hysteresis as well as an increase in advancing contact angle, the increase in surface roughness caused by the droplet formation after annealing of the l-CO_2 cast PFOEA film is not responsible for the increase of the contact angle hysteresis.

The increase in the contact angle hysteresis after annealing the l-CO_2 cast film may also be caused by the interaction between the test liquids and the native silicon oxide substrate in the open areas on the substrate.[48] The thickness of the polymer layers in the open areas is found to be very small; for example, after annealing the thickness of perfluorooctyl ethyl groups containing poly(methacrylate) is ~4.7 nm and that of perfluoroalkyl group containing poly(benzyl ether) groups is ~6 nm.[26,49] The Hamaker constant at the water(1)/PFOEA(3) interface (A_{13}) is 3.2×10^{-20} J, and the Hamaker constant for hydrocarbon-based test liquids (1′)/PFOEA(3) contacts is ($A_{1'3}$) is 3.7×10^{-20} J.[50] The effective Hamaker constant (A_{1324}) of the test liquids (1 or 1′)/PFOEA (3)/SiOx(2)/Si(4) can be estimated via the expression[51]

$$A_{1324} = (\sqrt{A_{33}} - \sqrt{A_{11}})(\sqrt{A_{33}} - \sqrt{A_{22}})\frac{(\sqrt{A_{33}} - \sqrt{A_{11}})(\sqrt{A_{33}} - \sqrt{A_{44}})}{(1 + \delta_{ox}/H)^3}$$

Here δ_{SiO} is the thickness of the native oxide layer (2 nm), and H is PFOEA film thickness (5 nm). The quantity A_{1324} is 0.53×10^{-20} J, and $A_{1'324}$ is 1.2×10^{-20} J. These values correspond to 16% of A_{13} and 32% of $A_{1'3}$. Thus, when the PFOEA films are ultrathin, the test liquids may "feel" the underlying silica substrate.

4. Conclusions

The surface characteristics of PFOEA films deposited by hFMC with l-CO_2 as coating solvent were compared to PFOEA films deposited by normal dip coating using Freon 113. Morphology measurement using AFM revealed that films deposited from l-CO_2 exhibits a terrace-like structure with a step height corresponding to one bilayer length of the polymer chain. Although the perfluoroalkyl chains were well-oriented normal to the substrate, the presence of the terrace-like structure leads to the exposure of carbonyl groups at the air/polymer interface. Annealing the films deposited from l-CO_2 and Freon 113 resulted in droplet formation due to dewetting. While the critical surface tensions (γ_c) of the films cast from Freon 113 increased from 6.5 mJ/m^2 (as-cast) to 8.5 mJ/m^2 (after annealing), the γ_c of films prepared from l-CO_2 decreased slightly from 9.7 mJ/m^2 (as-cast) to 8.9 mJ/m^2 (after annealing). This work reveals that surface morphology changes after annealing play an important role in the variation of γ_c in the as-cast and annealed samples.

Acknowledgment. This work was supported by the STC Program of the National Science Foundation under Agreement CHE-9876674. NEXAFS spectroscopy experiments were carried out at the National Synchrotron Light Source, Brookhaven National Laboratory, which is supported by the U.S. Department of Energy, Division of Materials Sciences and Division of Chemical Sciences. We thank Dr. Daniel A. Fischer (NIST) for his assistance during the course of the NEXAFS experiments.

References and Notes

(1) Wenzel, R. N. *J. Ind. Eng. Chem.* **1936**, *28*, 988−994.
(2) Dettre, R. H.; Johnson, R. E., Jr. In *Contact Angle, Wettability and Adhesion*; Gould, R. F., Ed.; American Chemical Society: Washington, DC, 1964; Advances in Chemistry Series Vol. 43, pp 136−144.
(3) Fabretto, M.; Sedev, R.; Ralston, J. In *Contact Angle, Wettability and Adhesion*; Mittal, K. L., Ed.; VSP: Boston, 2003, Vol. 3, pp 161−173.
(4) Luo, S. C.; Craciun, V.; Douglas, E. P. *Langmuir* **2005**, *21*, 2881−2886.
(5) Amautov, S. A.; Nechvolodova, E. M.; Bakulin, A. A.; Elizarov, S. G.; Khodarev, A.; Martyanov, D. S.; Paraschuk, D. Y. *Synth. Met.* **2004**, *147*, 287−291.
(6) Strawhecker, K. E.; Kumar, S. K.; Douglas, J. F.; Karim, A. *Macromolecules* **2001**, *34*, 4669−4672.
(7) Muller-Buschbaum, P.; Gutmann, J. S.; Wolkenhauer, M.; Kraus, J.; Stamm, M.; Smilgies, D.; Petry, W. *Macromolecules* **2001**, *34*, 1369−1375.
(8) Birnie, D. P. *J. Mater. Res.* **2001**, *16*, 1145−1154.
(9) de Gennes, P. G. *Eur. Phys. J. E* **2002**, *7*, 31−34.
(10) Kim, Jaehoon, Ph.D. Thesis, Deposition of Thin Organic and Metal Films from Carbon Dioxide by Free Meniscus and Solvent Displacement Methods, North Carolina State University, 2005.
(11) Volkov, V. V.; Plate, N. A.; Takahara, A.; Kajiyama, T.; Amaya, N.; Murata, Y. *Polymer* **1992**, *33*, 1316−1320.
(12) Kim, J.; Novick, B. J.; DeSimone, J. M.; Carbonell, R. G. *Langmuir* **2006**, *22*, 642−657.
(13) Novick, B. J.; DeSimone, J. M.; Carbonell, R. G. *Ind. Eng. Chem. Res.* **2004**, *43*, 515−524.
(14) Johnson, R. E., Jr.; Dettre, R. H. In *Wettability*; Berg, J. C., Ed.; Marcel Dekker: New York, 1993; Vol. 49, pp 1−73.
(15) Zisman, W. A. In *Contact Angle, Wettability and Adhesion*; Gould, R. F., Ed.; American Chemical Society: Washington, DC, 1964; Vol. 43, pp 1−51.
(16) Andrade, J. D. In *Surface and Interface Aspects of Biomedical Polymers: Surface Chemistry and Physics*; Andrade, J. D., Ed.; Plenum Press: New York, 1985; Vol. 1, pp 105−195.
(17) van Krevelen, D. W. *Properties of Polymers: Correlations with Chemical Structure*, 3rd ed.; Elsevier Pub. Co.: Amsterdam, 1990.
(18) Genzer, J.; Sivaniah, E.; Kramer, E. J.; Wang, J. G.; Korner, H.; Char, K.; Ober, C. K.; DeKoven, B. M.; Bubeck, R. A.; Fischer, D. A.; Sambasivan, S. *Langmuir* **2000**, *16*, 1993−1997.
(19) Genzer, J.; Sivaniah, E.; Kramer, E. J.; Wang, J. G.; Korner, H.; Xiang, M. L.; Char, K.; Ober, C. K.; DeKoven, B. M.; Bubeck, R. A.; Chaudhury, M. K.; Sambasivan, S.; Fischer, D. A. *Macromolecules* **2000**, *33*, 1882−1887.
(20) Stöhr, J. N*EXAFS Spectroscopy;* Springer: New York, 1996.
(21) Zharnikov, M.; Geyer, W.; Golzhauser, A.; Frey, S.; Grunze, M. *Phys. Chem. Chem. Phys.* **1999**, *1*, 3163−3171.
(22) Wirde, M.; Gelius, U.; Dunbar, T.; Allara, D. L. *Nucl. Instrum. Methods Phys. Res., Sect. B* **1997**, *131*, 245−251.
(23) Jager, B.; Schurmann, H.; Muller, H. U.; Himmel, H. J.; Neumann, M.; Grunze, M.; Woll, C. *Z. Phys. Chem. (Munich)* **1997**, *202*, 263−272.
(24) Soroka, A. J.; Tallmadge, J. A. *AIChE J.* **1971**, *17*, 505−508.
(25) Shimizu, T. In *Modern Fluoropolymers*; Scheirs, J., Ed.; John Wiley & Sons: Chichester, UK, 1997; pp 507−523.
(26) Sheiko, S.; Lermann, E.; Moeller, M. *Langmuir* **1996**, *12*, 4015−4024.
(27) Corpart, J. M.; Girault, S.; Juhue, D. *Langmuir* **2001**, *17*, 7237−7244.
(28) Park, I. J.; Lee, S.-B.; Choi, C. K.; Kim, K.-J. *J. Colloid Interface Sci.* **1996**, *181*, 284−288.
(29) Kassis, C. M.; Steehler, J. K.; Betts, D. E.; Guan, Z.; Romack, T. J.; DeSimone, J. M.; Linton, R. W. *Macromolecules* **1996**, *29*, 3247−3254.
(30) Carr, C.; Benjamin, S.; Walbridge, D. J. *Eur. Coat. J.* **1995**, *4*, 262−266.
(31) Verkholantsev, V.; Flavian, M. *Prog. Org. Coat.* **1996**, *29*, 239−246.
(32) Tsibouklis, J.; Stone, M.; Thorpe, A. A.; Graham, P.; Nevell, T. G.; Ewen, R. J. *Langmuir* **1999**, *15*, 7076−7079.
(33) Luning, J.; Yoon, D. Y.; Stöhr, J. *J. Electron Spectrosc. Relat. Phenom.* **2001**, *121*, 265−279.
(34) Luning, J.; Stöhr, J.; Song, K. Y.; Hawker, C. J.; Iodice, P.; Nguyen, C. V.; Yoon, D. Y. *Macromolecules* **2001**, *34*, 1128−1130.

(35) Ziegler, C.; Schedelniedrig, T.; Beamson, G.; Clark, D. T.; Salaneck, W. R.; Sotobayashi, H.; Bradshaw, A. M. *Langmuir* **1994**, *10*, 4399−4402.
(36) Castner, D. G.; Lewis, K. B.; Fischer, D. A.; Ratner, B. D.; Gland, J. L. *Langmuir* **1993**, *9*, 537−542.
(37) Ohta, T.; Seki, K.; Yokoyama, T.; Morisada, I.; Edamatsu, K. *Phys. Scr.* **1990**, *41*, 150−153.
(38) Hopken, J.; Sheiko, S.; Czech, J.; Moller, M. Polymer Surface Modification by Self-Organization of Fluorocarbon-Hydrocarbon Substituents. *Abstr. Pap. Am. Chem. Soc.* **1992**, *203*, 525.
(39) Gan, D. J.; Lu, S. Q.; Wang, Z. J. *J. Macromol. Sci., Phys.* **2001**, *40*, 199−206.
(40) vanderWielen, M. W. J.; Stuart, M. A. C.; Fleer, G. J.; deBoer, D. K. G.; Leenaers, A. J. G.; Nieuwhof, R. P.; Marcelis, A. T. M.; Sudholter, E. J. R. *Langmuir* **1997**, *13*, 4762−4766.
(41) Cho, K.; Cho, J. H.; Yoon, S.; Park, C. E.; Lee, J. C.; Han, S. H.; Lee, K. B.; Koo, J. *Macromolecules* **2003**, *36*, 2009−2014.
(42) Cassie, A. B. D.; Baxter, S. *Trans. Faraday Soc.* **1944**, *40*, 546−551.
(43) Cassie, A. B. D. *Discuss. Faraday Soc.* **1948**, *3*, 11−16.
(44) Marmur, A. *Soft Matter* **2006**, *2*, 12−17.
(45) Wolansky, G.; Marmur, A. *Colloids Surf., A* **1999**, *156*, 381−388.
(46) Johnson, R. E., Jr.; Dettre, R. H. In C*ontact Angle, Wettability and Adhesion;* Gould, R. F., Ed.; American Chemical Society: Washington, DC, 1964; Advances in Chemistry Series Vol. 43, pp 112−135.
(47) Tsibouklis, J.; Nevell, T. G. *Adv. Mater.* **2003**, *15*, 647−650.
(48) Ishikawa, M.; Morita, M.; Sakashita, H.; Kubo, M. *Polym. Prepr.* **1998**, *39*, 968−969.
(49) Gan, D.; Lu, S.; Wang, Z. *J. Macromol. Sci., Phys.* **2001**, *B40*, 199−206.
(50) Istraelachvili, J. N. In *Intermolecular and Surface Forces*; Academic Press: San Diego, CA, 1991; p 184. The Hamaker contant of water (1)/PFOEA (3) (A_{13}) was calculated using Lifshitz theory ($A_{33} = {}^3/_4 kT[(\epsilon_3 - 1)/(\epsilon_3 + 1)]^2 + (3h\nu_e)/(16\sqrt{2})(n_3{}^2 - 1)^2/(n_3{}^2 + 1)^{3/2}$) and combining raw ($A_{13} = \sqrt{A_{11}}\sqrt{A_{33}}$). Values to calculate A_{13} are as follows: $A_{11} = 3.7 \times 10^{-20}$ J, $A_{1'1'} = 5.0 \times 10^{-20}$ J, refractive index of PFOEA ($n_3 = 1.3$), and $\nu_e = 3 \times 10^{-15}$ s.
(51) Nir, S.; Vassilieff, C. S. In *Liquids at Interfaces*; Ivanov, I. B., Ed.; Marcell Dekker: New York, 1988; p 1126. Values to calculate A_{13} are as follows: $A_{22} = 6.5 \times 10^{-20}$ J, $A_{33} = 24 \times 10^{-20}$ J.
(52) Daubert, T. E.; Danner, R. P. D*ata Compilation Tables of Properties of Pure Compounds*; Daubert, T. E., Danner, R. P., Eds.; American Institute of Chemical Engineers: New York, 1985.
(53) Katano, Y.; Tomono, H.; Nakajima, T. *Macromolecules* **1994**, *27*, 2342−2344.
(54) Stone, M.; Nevell, T. G.; Tsibouklis, J. *Mater. Lett.* **1998**, *37*, 102−105.

MA0623791